Modelling dynamic processes in a nuclear reactor by state change modal method

A V Avvakumov[1], V F Strizhov[2], P N Vabishchevich[2,3] and A O Vasilev[3]

[1] National Research Center Kurchatov Institute, Moscow, Russia
[2] Nuclear Safety Institute of RAS, Moscow, Russia
[3] North-Eastern Federal University, Yakutsk, Russia

E-mail: haska87@gmail.com

Abstract. Modelling of dynamic processes in nuclear reactors is carried out, mainly, on the basis of the multigroup diffusion approximation for the neutron flux. The basic model includes a multidimensional set of coupled parabolic equations and ordinary differential equations. Dynamic processes are modelled by a successive change of the reactor states, which are characterized by given coefficients of the equations. It is considered that the transition from one state to another occurs instantaneously. In the modal method the approximate solution is represented as eigenfunction expansion. The numerical-analytical method is based on the use of dominant time-eigenvalues of a multigroup diffusion model taking into account delayed neutrons.

1. Introduction

These guidelines show how to prepare articles for publication in *Journal of Physics: Conference Series* using LaTeX so they can be published quickly and accurately. Articles will be refereed by the conference organizers but the accepted PDF will be published with no editing, proofreading or changes to layout. It is, therefore, the author's responsibility to ensure that the content and layout are correct. This document has been prepared using `jpconf.cls` so serves as a sample document. The class file and accompanying documentation are available from `http://jpcs.iop.org`. These guidelines show how to prepare articles for publication in *Journal of Physics: Conference Series* using LaTeX so they can be published quickly and accurately. Articles will be refereed by the conference organizers but the accepted PDF will be published with no editing, proofreading or changes to layout. It is, therefore, the author's responsibility to ensure that the content and layout are correct. This document has been prepared using `jpconf.cls` so serves as a sample document. The class file and accompanying documentation are available from `http://jpcs.iop.org`. These guidelines show how to prepare articles for publication in *Journal of Physics: Conference Series* using LaTeX so they can be published quickly and accurately. Articles will be refereed by the conference organizers but the accepted PDF will be published with no editing, proofreading or changes to layout. It is, therefore, the author's responsibility to ensure that the content and layout are correct. This document has been prepared using `jpconf.cls` so serves as a sample document. The class file and accompanying documentation are available from `http://jpcs.iop.org`.

2. Problem statement

The neutron flux is modelled in multigroup diffusion approximation. The neutron dynamics is considered in the bounded convex two-dimensional or three-dimensional area Ω ($\boldsymbol{x} = \{x_1, ..., x_d\} \in \Omega,\ d = 2, 3$) with boundary $\partial\Omega$. The neutron diffusion is described by:

$$\begin{gathered} V(t)\frac{d\boldsymbol{\phi}}{dt} + (D(t) + S(t))\boldsymbol{\phi} = R(t)\boldsymbol{\phi} + B(t)\boldsymbol{c}, \\ \frac{d\boldsymbol{c}}{dt} + \Lambda(t)\boldsymbol{c} = Q(t)\boldsymbol{\phi}. \end{gathered} \tag{1}$$

Where vectors $\boldsymbol{\phi} = \{\phi_1, \phi_2, ..., \phi_G\}$, $\boldsymbol{c} = \{c_1, c_2, ..., c_M\}$ and matrices:

$$\begin{gathered} V = (v_{gg'}), \quad v_{gg'} = \delta_{gg'} v_g^{-1}, \quad D = (d_{gg'}), \quad d_{gg'} = -\delta_{gg'}\nabla \cdot D_g \nabla, \\ S = (s_{gg'}), \quad s_{gg'} = \delta_{gg'}\Sigma_g - \Sigma_{s,g'\to g}, \quad R = (r_{gg'}), \quad r_{gg'} = (1-\beta)\chi_g \nu\Sigma_{fg'}, \\ B = (b_{gm}), \quad b_{gm} = \widetilde{\chi}_g \lambda_m, \quad \Lambda = (\lambda_{mm'}), \quad \lambda_{mm'} = \lambda_m \delta_{mm'}, \\ Q = (q_{mg}), \quad q_{mg} = \beta_m \nu\Sigma_{fg}, \quad g, g' = 1, 2, ..., G, \quad m, m' = 1, 2, ..., M, \end{gathered}$$

where $\delta_{gg'}$ is the Kronecker symbol. We shall use the set of vectors $\boldsymbol{\phi}$, whose components satisfy the albedo boundary conditions:

$$D_g \frac{\partial \phi_g}{\partial n} + \gamma_g \phi_g = 0, \qquad g = 1, 2, ..., G, \tag{2}$$

where n — outer normal to the boundary $\partial\Omega$.

Here $\phi_g(\boldsymbol{x}, t)$ — neutron flux of g group at point $\boldsymbol{x}$ and time t, G — number of energy groups, v_g — effective velocity of neutrons in the group g, $D_g(\boldsymbol{x})$ — diffusion coefficient, $\Sigma_{rg}(\boldsymbol{x}, t)$ — removal cross-section, $\Sigma_{s,g'\to g}(\boldsymbol{x}, t)$ — scattering cross-section from group g' to group g, β — effective fraction of delayed neutrons, χ_g, $\widetilde{\chi}_g$ — spectra of prompt and delayed neutrons, $\nu\Sigma_{fg}(\boldsymbol{x}, t)$ — generation cross-section of group g, c_m — density of sources of delayed neutrons of m-type, λ_m — decay constant of sources of delayed neutrons, M — number of types of delayed neutrons, and β_m is a fraction of delayed neutrons of m-type:

$$\beta = \sum_{m=1}^{M} \beta_m.$$

The Cauchy problem is formulated for equations (1) when

$$\boldsymbol{\phi}(0) = \boldsymbol{\phi}^0, \quad \boldsymbol{c}(0) = \boldsymbol{c}^0, \tag{3}$$

where taken into account $\boldsymbol{\phi}^0 = \{\phi_1^0, \phi_2^0, ..., \phi_G^0\}$, $\boldsymbol{c}^0 = \{c_1^0, c_2^0, ..., c_M^0\}$.

3. State change modal method

The nuclear reactor is always non-stationary. The limiting case of reaching a steady state (critical reactor) is observed only for certain coefficients of the equations system (1). We will use the following simplified description of the dynamic processes in a nuclear reactor.

In selected time interval, the non-stationary neutron flux is determined by the nuclear reactor state. The state of the reactor is characterized by the constant coefficients of the system of multigroup diffusion equations (1). Dynamic processes in a nuclear reactor can be considered as a change of states (see Fig.1). At a certain time $t = t_s,\ s = 1, 2, ...$ an instantaneous change of state occurs. The state s is defined by the parameters in equations (1):

$$V(t) = V(t_s), \quad D(t) = D(t_s), \quad S(t) = S(t_s), \quad R(t) = R(t_s), \quad B(t) = B(t_s),$$

$$\Lambda(t) = \Lambda(t_s), \quad Q(t) = Q(t_s), \quad t_{s-1} < t \le t_s, \quad s = 1, 2, ...$$

Simulation of the dynamic behavior of the reactor consists in solving the sequence of subtasks for the individual states of the reactor. The initial condition for the state s (at $t = t_{s-1}$) is the final state of the reactor for the state $s - 1$.

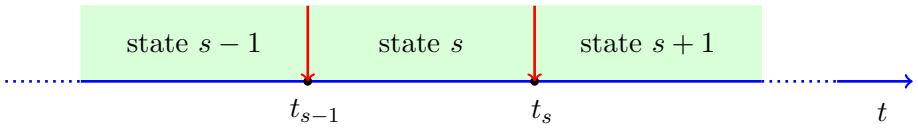

Figure 1. State change scheme.

An approximate description of the non-stationary process at a separate stage is based on modal approximation. An approximate solution is sought in the form of decomposition in eigenfunctions of time and α-eigenvalue problem. Finite-element approximation in space is used.

Let's $\boldsymbol{u} = \{\boldsymbol{\phi}, \boldsymbol{c}\}$. Rewrite the system of equations (1) as

$$\boldsymbol{B}\frac{d\boldsymbol{u}}{dt} + \boldsymbol{A}\boldsymbol{u} = 0, \quad t_{s-1} < t \le t_s, \tag{4}$$

with constants

$$\boldsymbol{A} = \begin{pmatrix} D(t_s) + S(t_s) - R(t_s) & -B(t_s) \\ -Q(t_s) & \Lambda(t_s) \end{pmatrix}, \quad \boldsymbol{B} = \begin{pmatrix} V(t_s) & 0 \\ 0 & I \end{pmatrix},$$

where I is the identity matrix. Initial conditions:

$$\boldsymbol{u}(t_{s-1}) = \boldsymbol{u}^s. \tag{5}$$

After approximating over the space by the finite element method from (4), (5) we turn to the Cauchy problem for a linear system of ordinary differential equations with constant coefficients:

$$\boldsymbol{B}_h\frac{d\boldsymbol{u}_h}{dt} + \boldsymbol{A}_h\boldsymbol{u}_h = 0, \quad t_{s-1} < t \le t_s, \tag{6}$$

$$\boldsymbol{u}_h(t_{s-1}) = \boldsymbol{u}_h^s, \tag{7}$$

where h is the discretization parameter. The main feature of the problems we are considering is that the matrices $\boldsymbol{A}_h$ and $\boldsymbol{B}_h$ are real and asymmetric.

The modal approximation corresponds to the representation of the approximate solution ($\boldsymbol{u}_h \approx \boldsymbol{u}_N$) of problem (6), (7) in the following form

$$\boldsymbol{u}_N(\boldsymbol{x}, t) = \sum_{n=1}^{N} a_n(t)\boldsymbol{w}_n(\boldsymbol{x}), \tag{8}$$

where N is the number of dominant eigenvalues of the spectral problem, $\boldsymbol{w}_n(\boldsymbol{x})$ — corresponding eigenfunctions.

Let us define eigenfunctions and eigenvalues as the solution of the α-eigenvalue problem:

$$\boldsymbol{A}_h\boldsymbol{v} = \lambda\boldsymbol{B}_h\boldsymbol{v}. \tag{9}$$

In the general case, eigenfunctions and eigenvalues of the spectral problem (9) are complex. Taking into account the validity of the matrix coefficients $\boldsymbol{A}_h,\ \boldsymbol{B}_h$ complex eigenvalues appear as pairs of complex conjugate numbers. For example, we have a pair of $n, n+1$:

$$\lambda_{n+1} = \mathrm{Re}\lambda_n - i\mathrm{Im}\lambda_n.$$

Then in the representation (8) we obtain

$$a_n(t)\boldsymbol{w}_n(\boldsymbol{x}) = b_n\mathrm{Re}\big(\exp(-\lambda_n(t-t_{s-1}))\boldsymbol{v}_n(\boldsymbol{x})\big),$$
$$a_{n+1}(t)\boldsymbol{w}_{n+1}(\boldsymbol{x}) = b_{n+1}\mathrm{Im}\big(\exp(-\lambda_n(t-t_{s-1}))\boldsymbol{v}_n(\boldsymbol{x})\big).$$

A special attention should be paid to define the coefficients $a_n(t_{s-1}) = b_n,\ n = 1, 2, ..., N$. For this, the initial condition (7) is involved. For example, in the case of real eigenvalues, we have

$$\boldsymbol{u}_h^s(\boldsymbol{x}) = \sum_{n=1}^{N_h} b_n\boldsymbol{v}_n(\boldsymbol{x}).$$

This representation is not very suitable for practical use with modal approximation, when we work only with dominant eigenfunctions.

The initial condition includes two components $\boldsymbol{u}_h^s(\boldsymbol{x}) = (\boldsymbol{\phi}_h^s(\boldsymbol{x}), \boldsymbol{c}_h^s(\boldsymbol{x}))$. Dynamic behaviour of these components is due to different time-scale processes. Delayed neutrons source determines slow processes, when $\boldsymbol{c}(\boldsymbol{x}, t)$ changes slightly with the reactor state change. In contrast, neutron flux $\boldsymbol{\phi}(\boldsymbol{x}, t)$ determines fast processes when the reactor state changes. By virtue of this separation of dynamic processes, we model the slow phase of the dynamics of the reactor with modal approximation and orientate ourselves on the approximate prediction of the initial state for delayed neutrons, only the function $\boldsymbol{c}_h^s(\boldsymbol{x})$ is approximated. The approximation $\boldsymbol{\phi}_h^s(\boldsymbol{x})$ is not of interest to us; we do not model a fast phase of the state change.

The standard approach for the decomposition of the function $\boldsymbol{u}_h^s(\boldsymbol{x})$ over the system of non-orthogonal functions $\boldsymbol{v}_n(\boldsymbol{x}),\ n = 1, 2, ..., N_h$ consists in using the biorthogonal system of functions [26, 9]. Consider the spectral problem adjoint to (9)

$$\boldsymbol{A}_h^T\widetilde{\boldsymbol{v}} = \lambda\boldsymbol{B}_h^T\widetilde{\boldsymbol{v}}. \tag{10}$$

The eigenfunctions of problems (9) and (10) are orthogonal [31, 40] in the sense of the equality

$$(\boldsymbol{B}_h\boldsymbol{v}_n, \widetilde{\boldsymbol{v}}_m) = 0, \quad m \neq n, \quad m, n = 1, 2, ..., N_h,$$

where $(\cdot, \cdot)$ means corresponding scalar product. In view of this, one can obtain

$$b_n = \frac{1}{(\boldsymbol{B}_h\boldsymbol{v}_n, \widetilde{\boldsymbol{v}}_n)}(\boldsymbol{u}_h^s, \boldsymbol{B}_h\widetilde{\boldsymbol{v}}_n), \quad n = 1, 2, ..., N_h. \tag{11}$$

With known solutions of the spectral problems (9), (10) the solution is represented in the form (8), (11).

In the approximate solution of problem (6), (7) only the first N coefficients b_n in (11) are used (see (8)):

$$\boldsymbol{c}_h^s(\boldsymbol{x}) \approx \sum_{n=1}^{N} b_n\boldsymbol{c}_n(\boldsymbol{x}), \tag{12}$$

where $\boldsymbol{v}_n(\boldsymbol{x}) = (\boldsymbol{\phi}_n(\boldsymbol{x}), \boldsymbol{c}_n(\boldsymbol{x}))$. In this case, the spectral problems (9), (10) are solved for N dominant eigenvalues. The solution of the adjoint spectral problem is involved only for calculating the initial condition coefficients.

The most favourable case – when we use single delayed neutron group — M = 1 (see 2). In common case we have to rely on the second level to distinguish fast and slow processes. Delayed neutrons groups differ in their characteristic times, which depnd on constants $\lambda_m, m = 1, 2, ..., M$ (see 2). At asymptotic stage the relatively slow processes prevail. It is due to the longest-lived delayed neutron precursor — the smallest $\lambda_m, m = 1, 2, ..., M$. Other groups are not taken into account using the modal approach.

The state change modal method is based on the following calculating scheme.

Off-line calculation. Calculation of the coefficients of the mathematical model of the multigroup diffusion approximation for the isolated reactor states, which is performed in advance. The status passport also includes calculated dominant eigenvalues and eigenfunctions of the α-eigenvalue problem (9). These data can be supplemented by dominant eigenvalues and eigenvalues of the conjugate eigenvalue problem (10).

On-line calculation. Real-time modeling is carried out on the basis of the modal solution of the problem (6), (7). The coefficients in the representation (12) are calculated from the initial condition using (11). The solution for other time intervals is determined according to (8).

4. The test: the dynamics of the VVER-1000 reactor during the transition from the supercritical mode to the subcritical mode

A test problem for a VVER-1000 reactor without a reflector [11] is considered in the two-dimensional approximation (Ω is a reactor core cross-section). A two-group approximation is used taken into account delayed neutrons.

4.1. General description

The geometric model of the VVER-1000 core consists of a set of hexagonal-shaped cassettes and is shown in Fig.2, where fuel assemblies of various types are shown. The assembly "wrench" size is 23.6 cm.

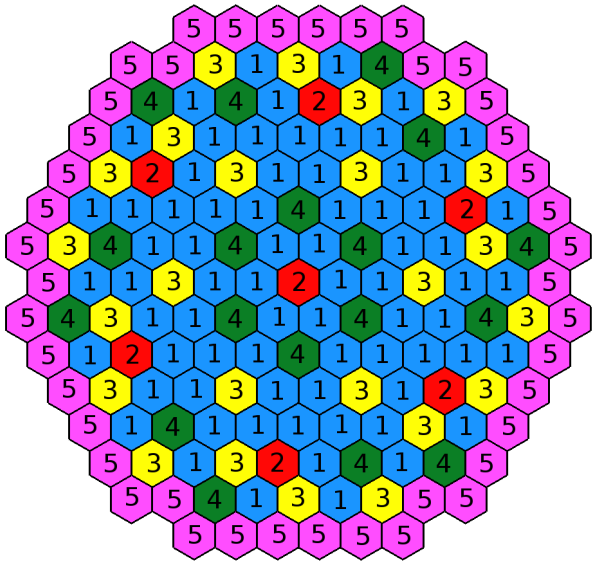

Figure 2. Geometrcial model of the VVER-1000 reactor core.

For an approximate solution of the problem, regular triangular grids are used. The number of triangles per cassette κ varies from 6 to 96.

Table 1. Diffusion neutronics constants for VVER-1000

Material	1	2	3	4	5
D_1	1.38320e-0	1.38299e-0	1.39522e-0	1.39446e-0	1.39506e-0
D_2	3.86277e-1	3.89403e-1	3.86225e-1	3.87723e-1	3.84492e-1
$\Sigma_1 + \Sigma_{s,1\to 2}$	2.48836e-2	2.62865e-2	2.45662e-2	2.60117e-2	2.46141e-2
Σ_2	6.73049e-2	8.10328e-2	8.44801e-1	9.89671e-2	8.93878e-2
$\Sigma_{s,1\to 2}$	1.64977e-2	1.47315e-2	1.56219e-2	1.40185e-2	1.54981e-2
$\nu\Sigma_{f1}$	4.81619e-3	4.66953e-3	6.04889e-3	5.91507e-3	6.40256e-3
$\nu\Sigma_{f2}$	8.46154e-2	8.52264e-2	1.19428e-1	1.20497e-1	1.29281e-1

The supercritical state of the reactor is characterized by a set of coefficients, which are given in Table 1. The following boundary conditions (3) are used: $\gamma_g = 0.5,\ g = 1, 2$. The following delayed neutrons parameters are used: one group of delayed neutrons with effective fraction $\beta_1 = 6.5 \cdot 10^{-3}$ and decay constant $\lambda_1 = 0.08\ \mathrm{s}^{-1}$. Neutron velocity $v_1 = 1.25 \cdot 10^7$ cm/s and $v_2 = 2.5 \cdot 10^5$ cm/s.

4.2. Supercritical state: α-eigenvalue problem

Below the results of a numerical solution of the α-eigenvalue problem (9) are presented. The dominant eigenvalues $\alpha_n = \lambda_n^{(\alpha)},\ n = 1, 2, ..., N$ are searched for at

$$\mathrm{Re}\lambda_1^{(\alpha)} \le \mathrm{Re}\lambda_2^{(\alpha)} \le ... \le \mathrm{Re}\lambda_N^{(\alpha)} \le ... \le \mathrm{Re}\lambda_{N_h}^{(\alpha)}.$$

Similar calculations of the eigenvalues for the VVER-1000 test problem without delayed neutrons can be found in [3].

Table 2. Eigenvalues $\alpha_n = \lambda_n^{(\alpha)},\ n = 1, 2, ..., 5$

p	κ	α_1	α_2, α_3	α_4, α_5
1	6	-0.22557	0.04241 $\mp$ 3.08808e-06i	0.06588 $\mp$ 4.80449e-07i
	24	-0.82690	0.03777 $\mp$ 5.37884e-06i	0.06489 $\mp$ 1.37315e-06i
	96	-1.74998	0.03619 $\mp$ 5.69002e-06i	0.06456 $\mp$ 1.40299e-06i
2	6	-2.10154	0.03592 $\mp$ 4.96474e-06i	0.06452 $\mp$ 1.21320e-06i
	24	-2.46601	0.03562 $\mp$ 5.78277e-06i	0.06445 $\mp$ 1.40897e-06i
	96	-2.50375	0.03559 $\mp$ 5.80693e-06i	0.06444 $\mp$ 1.41324e-06i
3	6	-2.47975	0.03561 $\mp$ 5.83718e-06i	0.06445 $\mp$ 1.41869e-06i
	24	-2.50294	0.03559 $\mp$ 5.80783e-06i	0.06444 $\mp$ 1.41341e-06i
	96	-2.51280	0.03558 $\mp$ 5.80954e-06i	0.06444 $\mp$ 1.41362e-06i

The results of solving the spectral problem (9) for the first eigenvalues $\alpha_n = \lambda_n^{(\alpha)},\ n = 1, 2, ..., N,\ N = 5$ on different computational grids using different finite element approximations

are shown in Table 2. The eigenvalues $\alpha_2, \alpha_3,\ \alpha_4, \alpha_5,\ \alpha_9, \alpha_{10}$ of the spectral problem (9) are complex with small imaginary parts, the eigenvalues $\alpha_1, \alpha_6,\ \alpha_7, \alpha_8$ are real.

In our example, the main eigenvalue is negative and therefore the major harmonic will increase, and all others will fade. This demonstrates the regular mode of the reactor operation. The value $\alpha = \lambda_1^{(\alpha)}$ itself determines the neutron flux amplitude and is directly related to the reactor period in the regular regime.

Table 3. Eigenvalues $\alpha_n = \lambda_n^{(\alpha)},\ n = 1, 2, ..., 10$ for direct and adjoint problems

n	α_n for problem (14)	α_n for problem (**??**)
1	-2.51280117966	-2.51280117972
2,3	0.0355815000364 ∓ 5.80954455861e-06	0.0355815000365 ∓ 5.80954421646e-06
4,5	0.0644427013767 ∓ 1.41362187449e-06	0.0644427013767 ∓ 1.41362190730e-06
6	0.0702618501639	0.0702618501639
7	0.0714652882224	0.0714652882164
8	0.0726456060606	0.0726456060606
9,10	0.0734708921578 ∓ 4.02332269037e-08	0.0734708921578 ∓ 4.02332146248e-08

4.3. Adjoint spectral problem

Analogous data were obtained for approximate solution of the adjoint spectral problem (10). The eigenvalues of the spectral problems (9) and (10) coincide. Their difference from each other is an indirect measure of the accuracy of the numerical solution. Data on the dominant eigenvalues, which are given in Table 3 ($k = 96,\ p = 3$), show that the eigenvalues of the main and adjoint spectral problems are close to each other with good accuracy.

The spectral problems under consideration are characterized by small imaginary parts of the eigenvalues. Therefore, we can expect that the eigenfunctions of problem (9) are close to orthogonal. As illustration, Table 4 contains data for the scalar products $(\phi_1^{(n)}, \phi_1^{(m)})$ for the first 10 eigenfunctions. For convenience of comparison, the eigenfunctions are normalized in $L_2(\Omega)$. The maximum non-orthogonality (for $(\phi_1^{(1)}, \phi_1^{(7)})$) does not exceed 10 %. The biorthogonality condition of the eigenfunctions of the fundamental functions (see (9)) and the adjoint spectral problems (see (10)) is valid with approximately the same accuracy. This observed error can be related to an approximate calculation of eigenvalues and eigenfunctions.

Within the modal method, we can not rely on high accuracy when considering a relatively small number of dominant eigenvalues. Therefore, in the example under consideration, we can assume that the eigenvalues are real, and the corresponding eigenfunctions are orthogonal. Instead of (11) coefficients are used

$$b_n \approx \frac{1}{(\boldsymbol{c}_n, \boldsymbol{c}_n)}(\boldsymbol{c}_h^s, \boldsymbol{c}_n), \quad n = 1, 2, ..., N, \tag{13}$$

to approximate the initial condition.

4.4. Subcritical state

In the supercritical mode, due to the sufficiently large magnitude of the main eigenvalue, the regular regime of the reactor is rapidly developing, where

$$\boldsymbol{u}(\boldsymbol{x}, t) \approx a_1 \exp(-\alpha_1 t)\boldsymbol{v}_1^0(\boldsymbol{x}).$$

Table 4. Scalar product $(\phi_1^{(n)}, \phi_1^{(m)})$, $n, m = 1, 2, ..., 10$

$n\backslash m$	1	2	3	4	5	6	7	8	9	10
1	1.0e-00	1.3e-08	2.2e-08	-3.8e-08	9.8e-09	-1.8e-09	1.0e-02	-3.2e-09	-2.2e-08	1.6e-09
2	1.3e-08	1.0e-00	-1.6e-08	-1.6e-08	1.4e-08	4.1e-08	1.2e-09	-2.0e-07	-3.1e-03	7.5e-03
3	2.2e-08	-1.6e-08	1.0e-00	-9.8e-09	-1.1e-08	-1.8e-08	1.1e-08	-3.3e-08	-7.5e-03	-3.1e-03
4	-3.8e-08	-1.6e-08	-9.8e-09	1.0e-00	-3.9e-10	-1.1e-08	1.4e-08	4.0e-09	3.0e-09	-1.1e-08
5	9.8e-09	1.4e-08	-1.1e-08	-3.9e-10	1.0e-00	2.9e-09	-1.6e-08	-1.9e-08	6.3e-09	6.3e-09
6	-1.8e-09	4.1e-08	-1.8e-08	-1.1e-08	2.9e-09	1.0e-00	-4.2e-09	-5.6e-03	4.1e-08	-1.2e-07
7	1.0e-02	1.2e-09	1.1e-08	1.4e-08	-1.6e-08	-4.2e-09	1.0e-00	-2.1e-09	-1.8e-08	8.0e-09
8	-3.2e-09	-2.0e-07	-3.3e-08	4.0e-09	-1.9e-08	-5.6e-03	-2.1e-09	1.0e-00	-5.2e-08	2.3e-07
9	-2.2e-08	-3.1e-03	-7.5e-03	3.0e-09	6.3e-09	4.1e-08	-1.8e-08	-5.2e-08	1.0e-00	-5.5e-07
10	1.6e-09	7.5e-03	-3.1e-03	-1.1e-08	6.3e-09	-1.2e-07	8.0e-09	2.3e-07	-5.5e-07	1.0e-00

Here $\boldsymbol{v}_1^0(\boldsymbol{x})$ is the first mode of the supercritical state. We consider the problem with the transition from this supercritical state at $t_0 = 0$ to the subcritical state.

The subcritical stage is characterized by a 15% increase in the coefficient Σ_2 for material 4 in the VVER-1000 test diffusion constants (see Table 1). Thus, the dynamics of the reactor is as follows:

$$\Sigma_2 \longrightarrow 1.15\Sigma_2 \quad \text{(material 4)}.$$

The initial state is characterized by specifying the initial conditions at $t_0 = 0$ as

$$\boldsymbol{u}(\boldsymbol{x}, 0) = \boldsymbol{v}_1^0(\boldsymbol{x}). \tag{14}$$

The calculational results of the dominant eigenvalues for the subcritical state are presented in Tables 5. In this case even the first eigenvalues not significantly differ from each other.

Table 5. Subcritical state: $\alpha_n = \lambda_n^{(\alpha)}$, $n = 1, 2, ..., 5$

p	κ	α_1	α_2, α_3	α_4, α_5
3	96	0.02122	$0.05376 \mp 2.20951\text{e-}06i$	$0.06763 \mp 1.04756\text{e-}06i$

For an approximate solution, we use the following formulation:

$$\boldsymbol{u}_N(\boldsymbol{x}, t) = \sum_{n=1}^{N} b_n \exp(-\mathrm{Re}\,\alpha_n\, t)\boldsymbol{v}_n(\boldsymbol{x}), \tag{15}$$

where the coefficients b_n, $n = 1, 2, ..., N$ are calculated according to the given initial condition (13). These coefficients for $N = 50$ are shown in Fig.3. As we see, an approximate solution can be described by first mode only.

We distinguish two phases of the dynamic process: fast and slow. In the fast phase, the initial condition (14) is rearranged to the initial condition, which corresponds to (15): from the function $\boldsymbol{u}(\boldsymbol{x}, 0)$ to the function $\boldsymbol{u}_N(\boldsymbol{x}, 0)$. The slow phase is associated with the evolution of

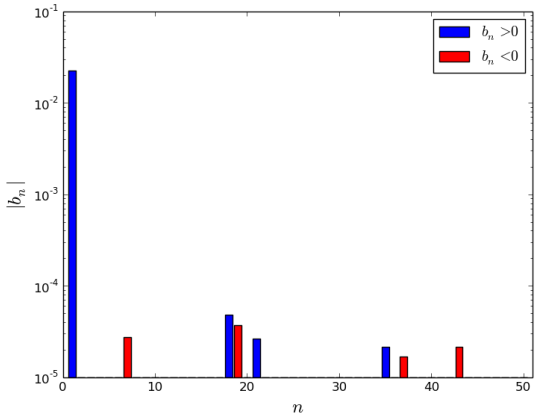

Figure 3. Approximate solution coefficients (15).

the solution according to (15). Within the state change modal technology, the fast phase is not modeled at all.

The beginning and the end of the fast phase are illustrated through the calculational data shown in Fig. 4. The results were obtained with $N = 10$. We can note very small changes in the topology of the initial and reconstructed initial conditions. Let us pay attention to the substantial restructuring of the solution, which is illustrated by large changes in the neutron flux amplitudes for the first and second groups.

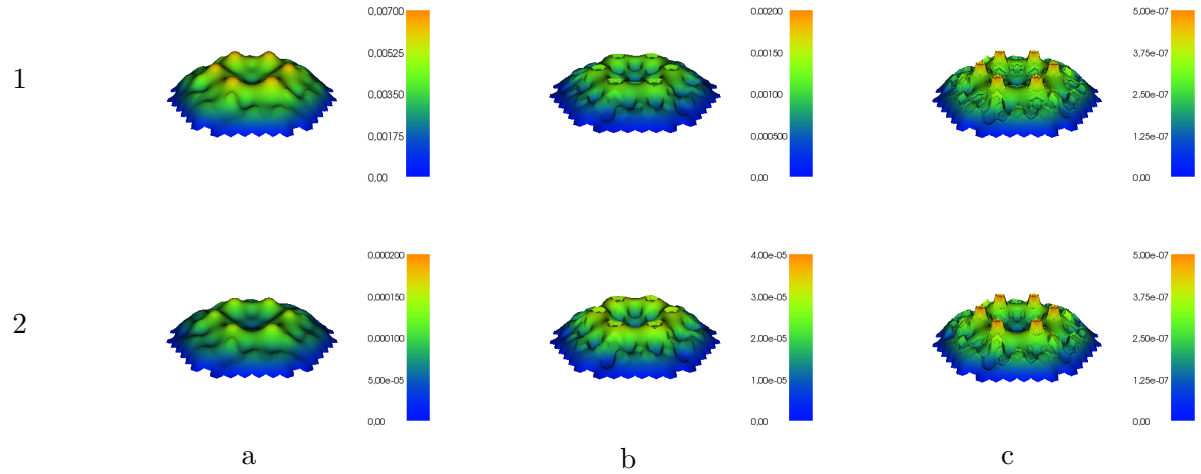

Figure 4. Function $\boldsymbol{u}(\boldsymbol{x}, 0)$ (string 1) and function $\boldsymbol{u}_N(\boldsymbol{x}, 0)$ (ctring 2): a — neutron flux of group 1, b — neutron flux of group 2, c — delayed neutrons source.

4.5. Comparison with the nonstationary problem solution

An approximate solution, obtained using modal approximation, can be compared with the dynamic problem solution (1). Fully implicit scheme on a uniform grid in time with a sufficiently small step $\tau = 0.0025$ is used (see details in [4]). The dynamics of the neutron power of the

nuclear reactor P and the delayed neutrons source C at the initial stage during the transition from the critical state to the subcritical in the case of a symmetric perturbation is shown in Fig.5. Here

$$P(t) = \int_\Omega (\nu\Sigma_{f1}\varphi_1 + \nu\Sigma_{f2}\varphi_2)d\boldsymbol{x}, \quad C(t) = \int_\Omega c(\boldsymbol{x}, t)d\boldsymbol{x}.$$

There is a rapid change in neutron power over a short period of time, while the delayed neutrons sourse changes rather slow. The dynamics of the slow phase is illustrated in Figs. 6. Here the solution of full equations (dynamic in Figs. 6), and the modal approximation solution (modal) are presented. We see that the integral characteristics of the reactor dynamics at slow stage are calculated with good accuracy.

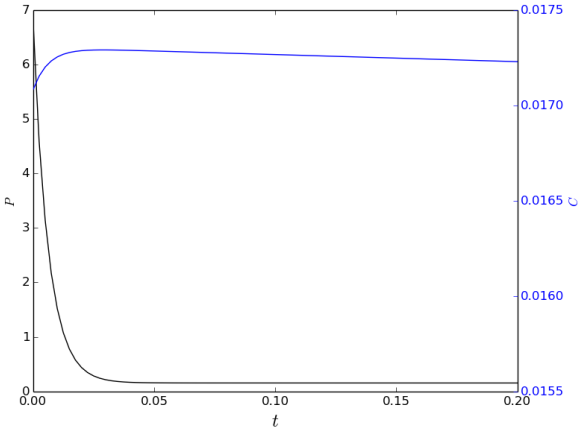

Figure 5. Fast stage of reactor state: neutronic power.

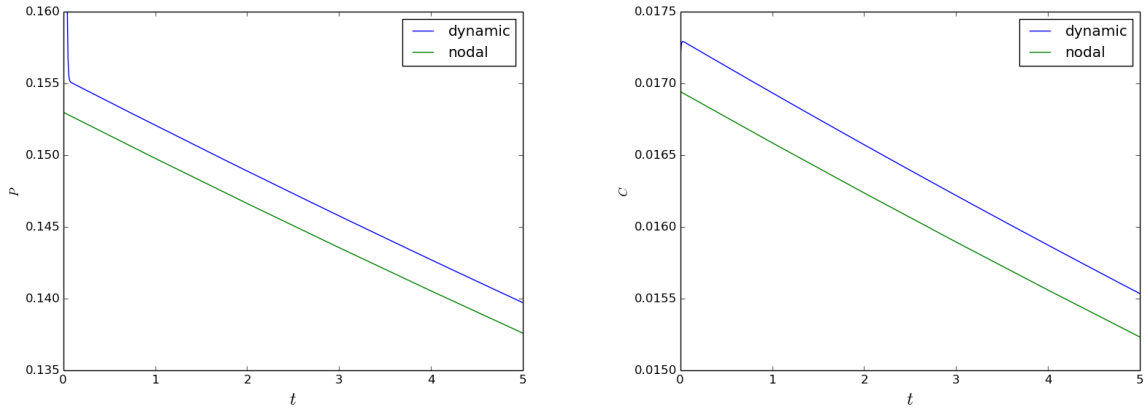

Figure 6. Slow stage of reactor state: neutronic power and delayed neutrons sourse

5. Conclusions

The problem of simulation of reactor dynamic processes is considered on the basis of multigroup neutron diffusion equations accounting for delayed neutrons. The modal approximation is used: an approximate solution is represented as an expansion on limited number of dominant eigenfunctions of the α-eigenvalue spectral problem.

Acknowledgements

This work are supported by the Russian Foundation for Basic Research (# 16-08-01215) and by the grant of the Russian Federation Government (# 14.Y26.31.0013).

References

[1] IOP Publishing is to grateful Mark A Caprio, Center for Theoretical Physics, Yale University, for permission to include the `iopart-num` BibTeXpackage (version 2.0, December 21, 2006) with this documentation. Updates and new releases of `iopart-num` can be found on `www.ctan.org` (CTAN).

[2] Ascher, U. M., 2008. Numerical Methods for Evolutionary Differential Equations. Society for Industrial Mathematics.

[3] Avvakumov, A. V., Strizhov, V. F., Vabishchevich, P. N., Vasilev, A. O., 2017. Spectral properties of dynamic processes in a nuclear reactor. Annals of Nuclear Energy 99, 68–79.

[4] Avvakumov, A. V., Vabishchevich, P. N., Vasilev, A. O., Strizhov, V. F., 2016. Numerical modelling neutron diffusion unsteady problems. Mathematical Models and Computer Simulations (submitted).

[5] Baudron, A.-M., Lautard, J.-J., Maday, Y., Riahi, M. K., Salomon, J., 2014. Parareal in time 3D numerical solver for the LWR benchmark neutron diffusion transient model. Journal of Computational Physics 279, 67–79.

[6] Bell, G. I., Glasstone, S., 1970. Nuclear Reactor Theory. Van Nostrand Reinhold Company.

[7] Bjrck, A., 1996. Numerical Methods for Least Squares Problems. Society for Industrial and Applied Mathematics.

[8] Brenner, S. C., Scott, R., 2008. The Mathematical Theory of Finite Element Methods. Springer.

[9] Brezinski, C., 1991. Biorthogonality and Its Applications to Numerical Analysis. CRC Press.

[10] Butcher, J. C., 2008. Numerical Methods for Ordinary Differential Equations. Wiley.

[11] Chao, Y. A., Shatilla, Y. A., 1995. Conformal mapping and hexagonal nodal methods-II: Implementation in the ANC-H Code. Nuclear Science and Engineering 121, 210–225.

[12] Cho, N. Z., 2005. Fundamentals and recent developments of reactor physics methods. Nuclear Engineering and Technology 37 (1), 25–78.

[13] Chou, H. P., Lu, J. R., Chang, M. B., 1990. A three-dimensional space-time model and its use in pressurized water reactor rod ejection analyses. Nuclear Technology 90 (2), 142–154.

[14] Dahmani, M., Baudron, A. M., Lautard, J. J., Erradi, L., 2001. A 3D nodal mixed dual method for nuclear reactor kinetics with improved quasistatic model and a semi-implicit scheme to solve the precursor equations. Annals of Nuclear Energy 28 (8), 805–824.

[15] Dodds Jr, H. L., 1976. Accuracy of the quasistatic method for two-dimensional thermal reactor transients with feedback. Nuclear Science and Engineering 59 (3), 271–276.

[16] Duderstadt, J. J., Hamilton, L. J., 1976. Nuclear Reactor Analysis. Wiley.

[17] Dugan, K., Zmijarevic, I., Sanchez, R., 2016. Cross-section homogenization for reactivity-induced transient calculations. Journal of Computational and Theoretical Transport 45 (6), 425–441.

[18] Dulla, S., Mund, E. H., Ravetto, P., 2008. The quasi-static method revisited. Progress in Nuclear Energy 50 (8), 908–920.

[19] Gear, C. W., 1971. Numerical Initial Value Problems in Ordinary Differential Equations. Prentice Hall, NJ.

[20] Ginestar, D., Miro, R., Verdu, G., Hennig, D., 2002. A transient modal analysis of a BWR instability event. Journal of Nuclear Science and Technology 39 (5), 554–563.

[21] Goluoglu, S., Dodds, H. L., 2001. A time-dependent, three-dimensional neutron transport methodology. Nuclear science and engineering 139 (3), 248–261.

[22] González-Pintor, S., Ginestar, D., Verdú, G., 2009. High order finite element method for the lambda modes problem on hexagonal geometry. Annals of Nuclear Energy 36 (9), 1450–1462.

[23] Grossman, L. M., Hennart, J.-P., 2007. Nodal diffusion methods for space-time neutron kinetics. Progress in Nuclear Energy 49 (3), 181–216.

[24] Guérin, P., Baudron, A.-M., Lautard, J.-J., 2010. Domain decomposition methods for the neutron diffusion problem. Mathematics and Computers in Simulation 80 (11), 2159–2167.

[25] Hairer, E., Wanner, G., 2010. Solving Ordinary Differential Equations II: Stiff and Differential-Algebraic Problems. Springer Verlag.
[26] Henry, A. F., 1975. Nuclear-Reactor Analysis. MIT press.
[27] Hernandez, V., Roman, J. E., Vidal, V., 2005. SLEPc: A scalable and flexible toolkit for the solution of eigenvalue problems. ACM Transactions on Mathematical Software (TOMS) 31 (3), 351–362.
[28] Hernandez, V., Roman, J. E., Vidal, V., Verdu, G., Ginestar, D., 2003. Resolution of the neutron diffusion equation with SLEPc, the Scalable Library for Eigenvalue Problem Computations. In: Nuclear Mathematical and Computational Sciences: A Century in Review, A Century Anew Gatlinburg. American Nuclear Society, pp. 1–10.
[29] Hetrick, D. L., 1971. Dynamics of Nuclear Reactors. University of Chicago Press.
[30] Hundsdorfer, W. H., Verwer, J. G., 2003. Numerical Solution of Time-Dependent Advection-Diffusion-Reaction Equations. Springer Verlag.
[31] Laub, A. J., 2005. Matrix Analysis for Scientists and Engineers. Society for Industrial and Applied Mathematics.
[32] Lawrence, R. D., 1986. Progress in nodal methods for the solution of the neutron diffusion and transport equations. Progress in Nuclear Energy 17 (3), 271–301.
[33] LeVeque, R. J., 2007. Finite Difference Methods for Ordinary and Partial Differential Equations: Steady-State and Time-Dependent Problems. Society for Industrial Mathematics.
[34] Lewis, E. E., Miller, W. F., 1993. Computational Methods of Neutron Transport. American Nuclear Society.
[35] Luikov, A., 1968. Analytical Heat Diffusion Theory. Academic Press.
[36] Maday, Y., Turinici, G., 2005. The parareal in time iterative solver: a further direction to parallel implementation. In: Domain Decomposition Methods in Science and Engineering. Springer, pp. 441–448.
[37] Marchuk, G. I., Lebedev, V. I., 1986. Numerical Methods in the Theory of Neutron Transport. Harwood Academic Pub.
[38] Miró, R., Ginestar, D., Verdú, G., Hennig, D., 2002. A nodal modal method for the neutron diffusion equation. application to BWR instabilities analysis. Annals of Nuclear Energy 29 (10), 1171–1194.
[39] Modak, R., Gupta, A., 2007. A scheme for the evaluation of dominant time-eigenvalues of a nuclear reactor. Annals of Nuclear Energy 34 (3), 213–221.
[40] Ortega, J. M., 1987. Matrix Theory: A Second Course. Springer.
[41] Quarteroni, A., Valli, A., 2008. Numerical Approximation of Partial Differential Equations. Springer.
[42] Saad, Y., 2003. Iterative Methods for Sparse Linear Systems. Society for Industrial Mathematics.
[43] Saad, Y., 2011. Numerical Methods for Large Eigenvalue Problems. SIAM.
[44] Samarskii, A. A., 2001. The Theory of Difference Schemes. Marcel Dekker, New York.
[45] Samarskii, A. A., Vabishchevich, P. N., 1996. Computational Heat Transfer. Wiley.
[46] Sanchez, R., 2009. Assembly homogenization techniques for core calculations. Progress in Nuclear Energy 51 (1), 14–31.
[47] Smith, K. S., 1979. An analytic nodal method for solving the two-group, multidimensional, static and transient neutron diffusion equations. Ph.D. thesis, Massachusetts Institute of Technology.
[48] Stacey, W. M., 1967. Modal Approximations: Theory and an Application to Reactor Physics. The MIT Press.
[49] Stacey, W. M., 1969. Space-Time Nuclear Reactor Kinetics. Academic Press.
[50] Stacey, W. M., 2007. Nuclear Reactor Physics. Wiley.
[51] Stewart, G. W., 2001. A Krylov–Schur algorithm for large eigenproblems. SIAM Journal on Matrix Analysis and Applications 23 (3), 601–614.
[52] Stewart, H. B., 1976. Spectral theory of heterogeneous diffusion systems. Journal of Mathematical Analysis and Applications 54 (1), 59–78.
[53] Sutton, T. M., Aviles, B. N., 1996. Diffusion theory methods for spatial kinetics calculations. Progress in Nuclear Energy 30 (2), 119–182.
[54] Toselli, A., Widlund, O., 2005. Domain Decomposition Methods – Algorithms and Theory. Springer.
[55] Vabishchevich, P. N., 2012. SM-stability of operator-difference schemes. Computational Mathematics and Mathematical Physics 52 (6), 887–894.
[56] Vabishchevich, P. N., 2014. Additive Operator-Difference Schemes: Splitting Schemes. de Gruyter.
[57] Verdú, G., Ginestar, D., 2014. Modal decomposition method for BWR stability analysis using Alpha-modes. Annals of Nuclear Energy 67, 31–40.
[58] Verdu, G., Ginestar, D., Roman, J., Vidal, V., 2010. 3D alpha modes of a nuclear power reactor. Journal of Nuclear Science and Technology 47 (5), 501–514.
[59] Verdú, G., Ginestar, D., Vidal, V., Miró, R., 1998. Modal decomposition method for BWR stability analysis. Journal of Nuclear Science and Technology 35 (8), 538–546.
[60] Vidal-Ferrandiz, A., Fayez, R., Ginestar, D., Verdú, G., 2014. Solution of the lambda modes problem of a

nuclear power reactor using an h–p finite element method. Annals of Nuclear Energy 72, 338–349.